

How much room for BiGa heteroantites in GaAs_{1-x}Bi_x ?

G. Ciatto, P. Alippi, A. Amore Bonapasta, and T. Tiedje

Citation: [Applied Physics Letters](#) **99**, 141912 (2011); doi: 10.1063/1.3647635

View online: <http://dx.doi.org/10.1063/1.3647635>

View Table of Contents: <http://scitation.aip.org/content/aip/journal/apl/99/14?ver=pdfcov>

Published by the [AIP Publishing](#)

Articles you may be interested in

[Identification of an isolated arsenic antisite defect in GaAsBi](#)

Appl. Phys. Lett. **104**, 052110 (2014); 10.1063/1.4864644

[Antisites and anisotropic diffusion in GaAs and GaSb](#)

Appl. Phys. Lett. **103**, 142107 (2013); 10.1063/1.4824126

[X-ray diffraction analysis of the structure of antisite arsenic point defects in low-temperature-grown GaAs layer](#)

J. Appl. Phys. **101**, 073513 (2007); 10.1063/1.2715523

[Lattice parameter and hole density of \(Ga,Mn\)As on GaAs\(311\)A](#)

Appl. Phys. Lett. **88**, 051904 (2006); 10.1063/1.2170408

[Native hole traps of ferromagnetic Ga_{1-x}Mn_xAs layers on \(100\) GaAs substrates](#)

Appl. Phys. Lett. **83**, 4354 (2003); 10.1063/1.1629398

HIDEN
ANALYTICAL

Instruments for Advanced Science

Contact Hiden Analytical for further details:

www.HidenAnalytical.com

info@hiden.co.uk

[CLICK TO VIEW](#) our product catalogue



Gas Analysis

- › dynamic measurement of reaction gas streams
- › catalysis and thermal analysis
- › molecular beam studies
- › dissolved species probes
- › fermentation, environmental and ecological studies



Surface Science

- › UHV TPD
- › SIMS
- › end point detection in ion beam etch
- › elemental imaging - surface mapping



Plasma Diagnostics

- › plasma source characterization
- › etch and deposition process reaction
- › kinetic studies
- › analysis of neutral and radical species



Vacuum Analysis

- › partial pressure measurement and control of process gases
- › reactive sputter process control
- › vacuum diagnostics
- › vacuum coating process monitoring

How much room for Bi_{Ga} heteroantisites in GaAs_{1-x}Bi_x?

G. Ciatto,^{1,a)} P. Alippi,² A. Amore Bonapasta,² and T. Tiedje³

¹Synchrotron SOLEIL, L'Orme des Merisiers, Saint-Aubin, BP48, Gif-sur-Yvette Cedex 91192, France

²CNR-Istituto di Struttura della Materia, Via Salaria km. 29, Monterotondo Stazione 300 I-00016, Italy

³Department of Electrical and Computer Engineering, University of Victoria, Victoria, British Columbia V8W 3P6, Canada

(Received 5 August 2011; accepted 12 September 2011; published online 6 October 2011)

We addressed the issue of bismuth heteroantisite defects (Bi_{Ga}) in GaAs_{1-x}Bi_x/GaAs epilayers by coupling x-ray absorption spectroscopy at the bismuth edge with density functional theory calculations of the defect structure. Calculations predict a large relaxation of the Bi-As interatomic distances when Bi atoms substitute Ga, however we found no experimental evidence of it. Quantitative analysis of the x-ray absorption spectra allows us to establish a maximum concentration limit for Bi_{Ga}, which corresponds to about 5% of the total Bi atoms. Bi_{Ga} do not account for the modifications in the spectra previously attributed to short range ordering. © 2011 American Institute of Physics. [doi:10.1063/1.3647635]

Dilute bismuthides such as GaAs_{1-x}Bi_x and GaAs_{1-x-y}Bi_xN_y ($x < 0.1$ and $y < 0.02$) are an innovative class of semiconductor alloys with enormous potential applications in different fields of technology. Alloying GaAs with Bi produces a giant reduction of the optical band gap, which makes these materials interesting for the manufactory of lasers and solar cell components in the infrared region.^{1,2} Moreover, since the incorporation of Bi on the anion site, at odds with N, perturbs only the valence band of GaAs,^{3,4} electron transport properties in GaAs_{1-x}Bi_x are less affected than in GaAs_{1-x}N_x.⁵ Finally, a strong enhancement of spin-orbit splitting⁶ makes GaAs_{1-x}Bi_x promising for the design of spintronic devices.

On the other hand, the electronic structure of dilute bismuthides is not well understood yet. It has been recently shown that the exciton reduced mass has a surprising compositional dependence: it anomalously increases for $x < 5\%$, while for $x > 5\%$ it decreases and begins following a conventional behavior.⁷ More recently, far-infrared absorption measurements have revealed the presence of acceptor states related to Bi, exclusively in the low-concentration “anomalous” region;⁸ the physical origin of these acceptors remains still an open question.

The anomalous optical and electronic properties of GaAs_{1-x}Bi_x cannot be accounted for assuming a virtual crystal in which Bi atoms simply substitute the isovalent As ones (Bi_{As}), and possible deviations from such an ideal situation have been examined by different experimental techniques. Extended x-ray absorption fine structure (EXAFS) spectroscopy⁹ allowed us to give evidence of short range ordering (SRO) of Bi atoms for $x < 2.5\%$,^{10,11} while Norman *et al.* have detected CuPt_B-type ordering¹² and coarser phase separation for different concentration ranges via transmission electron microscopy. Sales *et al.*,¹³ performing Z-contrast images, have also shown that the distribution of Bi atoms in GaAs_{1-x}Bi_x differs from a random spatial pattern.

A still rather unaddressed point, instead, is whether Bi atoms can possess valence different from five and/or occupy Ga lattice sites (heteroantisite defects, Bi_{Ga}). As a matter of

fact, because of the large energy separation between 6s and 6p orbitals related to the large relativistic effects in heavy atoms,¹⁴ valence three is *a priori* possible for Bi and, at the same time, Bi_{Ga} have been already observed at the Bi dilute limit by electron spin resonance (ESR).¹⁵ Bi_{Ga} have been also invoked as possible acceptor compensators to explain the reduction in the effective hole concentration observed upon Bi incorporation.¹⁶ The possibility of Bi multivalency and multisite occupancy would enable four different impurity configurations: isovalent impurity and double acceptor for Bi_{As} and isovalent impurity and double donor for Bi_{Ga}. Finally, the presence of a non-negligible fraction of Bi_{Ga} defects could affect the determination of SRO done by EXAFS.¹⁰ Hence, there are several important reasons for understanding if Bi_{Ga} defects actually exist in the Bi concentration range of interest for technological applications and for determining their atomic fraction.

In this work, EXAFS at the Bi L2-edge and density functional theory (DFT) calculations are coupled to study quantitatively the lattice location of Bi in GaAs_{1-x}Bi_x, in particular addressing the structure of Bi_{Ga} defects. DFT calculations predict a large relaxation of the Bi-As interatomic distances in the case of Bi_{Ga}, which is not observed experimentally. In fact, the introduction of Bi_{Ga} in the EXAFS fitting model does not improve the agreement with the experimental data. We establish the maximum concentration limit for Bi_{Ga} to be $\approx 5\%$ of the total Bi atoms in the alloy: this value is smaller than that determined previously at the Bi dilute limit.¹⁵ We also clarify that Bi_{Ga} cannot reproduce the variations in EXAFS spectra observed with increasing Bi concentration and previously attributed to SRO.¹⁰

We investigated the same three molecular beam epitaxy-grown Ga_{1-x}Bi_x epilayers addressed in our previous paper.¹⁰ We refer to this work and to references therein for details on the sample growth, the optical/structural characterization and the EXAFS setup. Sample characteristics are summarized in Table I. DFT calculations of relaxed geometries of substitutional Bi both on the As and Ga site have been performed within the projector augmented wave method and the Heyd-Scuseria-Ernzerhof (HSE) hybrid

^{a)}Electronic mail: gianluca.ciatto@synchrotron-soleil.fr.

TABLE I. Samples characteristics and fit results. Bi concentration was measured with RBS, film thickness was obtained by XRD simulations and RBS profiles, Bi_{Ga} fraction was extracted by fitting the EXAFS data.

Bi concentration (%)	Thickness (nm)	Bi_{Ga} fraction (%)
1.2	270 ± 15	0.2 ± 5.0
1.9	210 ± 10	1.4 ± 4.5
2.4	210 ± 10	2.9 ± 6.0

density functional¹⁷ as implemented in the Vienna *ab-initio* Simulation Package.¹⁸ Following a procedure already exploited in previous works,^{10,19,20} clusters of about 400 atoms centered on Bi_{As} and Bi_{Ga} have been build up from relaxed DFT geometries²¹ and further given as input of the FEFF code,²² in order to calculate the EXAFS theoretical signals exploited in the data analysis. Theoretical $\chi(k)$ signals were finally k^2 -weighted and Fourier transformed together with the experimental ones.

The local relaxed geometries of Bi_{As} and Bi_{Ga} given by DFT calculations are sketched in Fig. 1. In both cases, substitutional Bi induces significant outward relaxations of its 1st-neighbors positions. However, nearest-neighbor (NN) Bi-As distances (2.78 Å) in the Bi_{Ga} configuration are sensibly larger than NN Bi-Ga ones (2.63 Å) for Bi substituting the As site. NN distances have to be compared in both cases to the calculated Ga-As bulk bond length of 2.46 Å. 2nd shell distances are instead similar in the two structures. We calculate a larger formation energy for Bi_{Ga} configuration with respect to Bi_{As} , the difference being some eV for any reasonable choice of the chemical potentials. Our calculations describe Bi as isovalent anion when substituting As, ruling out the double acceptor behavior. On the other hand, Bi as a cation on the Ga site is a double-donor impurity, inducing a doubly occupied gap-state roughly located 0.2 eV above the valence band top. Bi_{Ga} 5+ oxidation state leaves around two excess electrons that, acting as an excess charge on the Bi site, induce large repulsive interactions with NN As atoms. This explains the larger Bi-NN relaxations occurring in the Bi_{Ga} configuration with respect to Bi_{As} , as well as its higher formation energy. We point out here that, owing to the small difference in atomic number between Ga and As, there is no

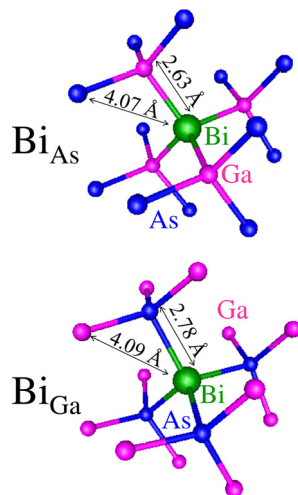


FIG. 1. (Color online) Sketch of Bi_{As} and Bi_{Ga} configurations.

chance to discriminate a Bi-Ga EXAFS contribution from a Bi-As one if Ga and As are located at the same distance from Bi. Hence, DFT calculations, predicting Bi-Ga from Bi-As distances to be different by 0.15 Å play a fundamental role in this study.

Fig. 2 shows the Fourier transformed Bi L2-edge EXAFS spectrum (modulus and imaginary part) for a relatively low concentration sample ($x = 1.2\%$), which is the most suitable for the present analysis since no short range ordering of Bi atoms is supposed to exist here according to our previous work.¹⁰ The experimental spectrum (continuous line) is very well reproduced by the simulation for the Bi_{As} configuration (circles). On the other hand, the simulation for the Bi_{Ga} (dashed line) gives strong disagreement with the data, in particular on the 1st shell peak where the predicted 1st-neighbors distance is sensibly longer than the measured one. We point out that in these simulations all interatomic distances were fixed to the values determined by DFT calculations, while Debye-Waller factors (DWs) and the edge energy shift (ΔE) were fixed to the values determined previously via an independent analysis method,¹⁰ the amplitude factor S_0^2 of the overall EXAFS signal was determined by the fit of a Bi foil. In other words, we used no variable when performing these fits employing the Artemis code.²³ If variable DWs are allowed while fitting with the Bi_{Ga} model, extremely high (and not realistic) values for the 1st shell Bi-As DWs are obtained, which causes a complete disappearance of the 1st shell peak in the simulated spectrum (not shown). This result gives already a clear indication that Bi heteroantisites, if existing, represent a minority configuration compared to Bi_{As} .

In order to determine how much room is available for Bi_{Ga} , we performed fits of the experimental spectra by combining the Bi_{As} and Bi_{Ga} configurations. The only variable used in these fits is the relative percentage of the two structures, being all the other parameters fixed as in the

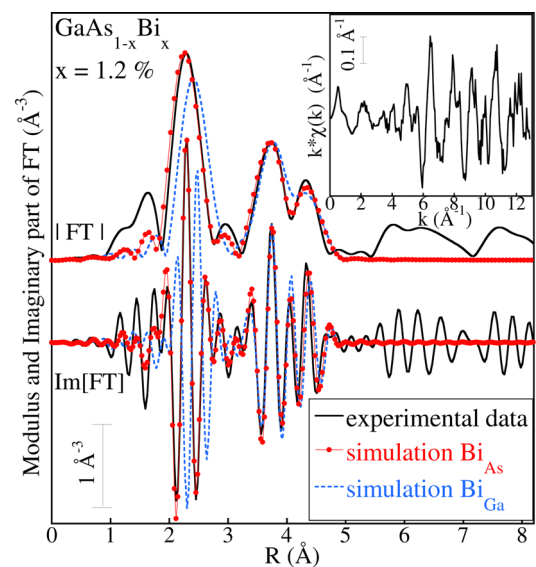


FIG. 2. (Color online) FT of the Bi L2-edge EXAFS spectrum for the $x = 1.2\%$ sample (continuous line) along with simulations performed for the Bi_{As} (circles) and Bi_{Ga} (dashed line) configurations. FT modulus is vertically shifted with respect to the FT imaginary part for better visualization. Δk interval for the FT was $[3.2-12.4 \text{ \AA}^{-1}]$, $\Delta E = 3.71 \text{ eV}$. Inset: background subtracted $k * \chi(k)$ spectrum.

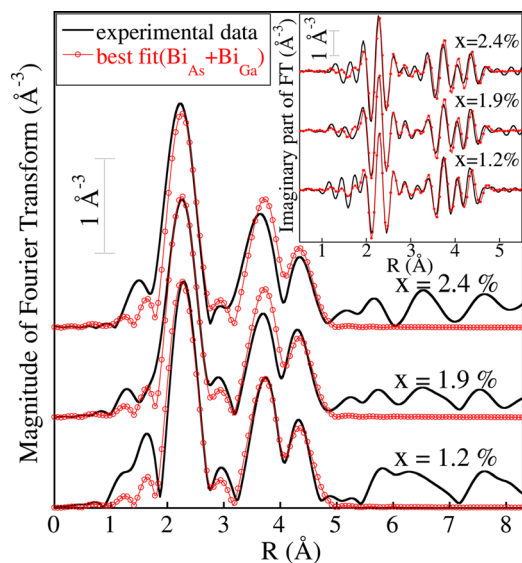


FIG. 3. (Color online) Magnitude of FT of the Bi L2-edge EXAFS spectra for the three samples (continuous line) along with best fits (open circles) obtained combining the Bi_{As} and Bi_{Ga} configurations. $\Delta k = [3.2\text{--}12.4 \text{ \AA}^{-1}]$, $\Delta E = 3.71 \text{ eV}$. Inset: imaginary part of the FT (data and fits).

simulations reported in Fig. 2. The minimization of the number of variables annuls correlation effects and increases the degrees of freedom: this strategy was chosen to minimize the error bars on the extracted Bi_{Ga} fractions. The fit performed on the $x = 1.2\%$ sample combining Bi_{As} and Bi_{Ga} is shown in Fig. 3 (lowest spectrum). The best fit is obtained for a percentage of $\text{Bi}_{\text{Ga}} = 0.2\% \pm 5.0\%$, which means that the estimated fraction of Bi_{Ga} defects does not differ from zero within the experimental uncertainty. From the 1σ error bar of the fit, it is possible to estimate the maximum concentration limit allowed for Bi_{Ga} in the sample, which corresponds to about 5.0% of the total Bi atoms. This limit is smaller than that previously determined via ESR for lower concentration samples,¹⁵ and excludes any possible increasing trend of antisite fraction with Bi concentration. Therefore, it is unlikely that the reduction of effective hole concentration observed for increasing Bi content is caused by Bi_{Ga} .¹⁶ The small (if existing) fraction of Bi_{Ga} agrees with the larger DFT formation energy calculated for this configuration with respect to Bi_{As} , as discussed above.

We applied the same fit strategy based on the combination of the Bi_{As} and Bi_{Ga} configurations in the analysis of two other samples with concentrations $x = 1.9\%$ and 2.4% , where SRO of Bi atoms was previously detected,¹⁰ in order to understand if the presence of a larger concentration of Bi_{Ga} can alternatively account for the differences observed in the Fourier-transformed EXAFS spectra with respect to the $x = 1.2\%$ one. Best fits, performed assuming *random* distribution of Bi atoms, are also reported in Fig. 3 (two upper spectra). The extracted Bi_{Ga} defect fractions are reported in Table I together with that of the $x = 1.2\%$ sample. It is clear from the figure and the table that introducing a fraction of Bi_{Ga} in the fit model does not lead to an improved agreement with the experimental data on the 2nd shell peak of the Fourier transform, and best fits obtained in this way for the $x = 1.9\%$ and 2.4% samples are not satisfactory. Hence, the

$\text{Bi}_{\text{As}} + \text{Bi}_{\text{Ga}}$ model does not describe well the distribution of atoms in the lattice for these two samples, and the low fraction of Bi heteroantisite defects possibly present cannot affect the determination of SRO reported previously.¹⁰

In conclusion, based on DFT calculations and quantitative analysis of Bi L2-edge EXAFS data, we find no evidence of the presence of Bi heteroantisites in $\text{GaAs}_{1-x}\text{Bi}_x$ in the concentration range 1.2% to 2.4%, and we estimate that the maximum allowed concentration for these defects corresponds to about 5% of the total Bi atoms. Our results are in agreement with those of a recent Z-contrast microscopy experiment, which has suggested that antisite bonding is inexistent in similar samples.¹³ Bi multivalency or multisite occupancy are not at the origin of the anomalous electronic properties of these materials,^{7,8,16} which might be explained by some type of short range ordering^{10–12} or other defects.

We acknowledge the European Synchrotron Radiation Facility for funding through Project Nos. MA237 and MA436. We are grateful to A. Polimeni for useful discussion.

- ¹T. Tiedje, E. C. Young, and A. Mascarenhas, *Int. J. Nanotechnol.* **5**, 963 (2008).
- ²X. Lu, D. A. Beaton, R. B. Lewis, T. Tiedje, and Y. Zhang, *Appl. Phys. Lett.* **95**, 041903 (2009).
- ³A. Janotti, S. H. Wei, and S. B. Zhang, *Phys. Rev. B* **65**, 115203 (2002).
- ⁴Y. Zhang, A. Mascarenhas, and L. W. Wang, *Phys. Rev. B* **71**, 155201 (2005).
- ⁵D. G. Cooke, E. C. Young, F. A. Hegmann, and T. Tiedje, *Appl. Phys. Lett.* **89**, 122103 (2006).
- ⁶B. Fluegel, S. Francoeur, A. Mascarenhas, S. Tixier, E. C. Young, and T. Tiedje, *Phys. Rev. Lett.* **97**, 067205 (2006).
- ⁷G. Pettinari, A. Polimeni, J. H. Blokland, R. Trotta, P. C. Christiansen, M. Capizzi, J. C. Maan, X. Lu, E. Young, and T. Tiedje, *Phys. Rev. B* **81**, 235211 (2010).
- ⁸G. Pettinari, H. Engelkamp, P. C. M. Christianen, J. C. Maan, A. Polimeni, M. Capizzi, X. Lu, and T. Tiedje, *Phys. Rev. B* **83**, 201201(R) (2011).
- ⁹C. Lamberti, *Surf. Sci. Rep.* **53**, 1 (2004).
- ¹⁰G. Ciatto, E. C. Young, F. Glas, J. Chen, R. A. Mori, and T. Tiedje, *Phys. Rev. B* **78**, 035325 (2008).
- ¹¹G. Ciatto, M. Thomasset, F. Glas, X. Lu, and T. Tiedje, *Phys. Rev. B* **82**, 201304 (2010).
- ¹²A. G. Norman, R. France, and A. J. Ptak, *J. Vac. Sci. Technol. B* **29**, 03C121 (2011).
- ¹³D. L. Sales, E. Guerrero, J. F. Rodrigo, P. L. Galindo, A. Yez, M. Shafi, A. Khatab, R. H. Mari, M. Henini, S. Novikov, M. F. Chisholm, and S. I. Molina, *Appl. Phys. Lett.* **98**, 101902 (2011).
- ¹⁴H.-X. Deng, J. Li, S.-S. Li, H. Peng, J.-B. Xia, L.-W. Wang, and S.-H. Wei, *Phys. Rev. B* **82**, 193204 (2010).
- ¹⁵M. Kunzer, W. Jost, U. Kaufmann, H. M. Hobgood, and R. N. Thomas, *Phys. Rev. B* **48**, 4437 (1993).
- ¹⁶R. N. Kini, A. J. Ptak, B. Fluegel, R. France, R. C. Reedy, and A. Mascarenhas, *Phys. Rev. B* **83**, 075307 (2011).
- ¹⁷J. Heyd, G. E. Scuseria, and M. Ernzerhof, *J. Chem. Phys.* **124**, 219906 (2006).
- ¹⁸G. Kresse and J. Furthmüller, *Phys. Rev. B* **54**, 11169 (1996).
- ¹⁹G. Ciatto, J.-C. Harmand, F. Glas, L. Largeau, M. Le Du, F. Boscherini, M. Malvestuto, L. Floreano, P. Glatzel, and R. Alonso Mori, *Phys. Rev. B* **75**, 245212 (2007).
- ²⁰G. Ciatto, A. Di Trolio, E. Fonda, P. Alippi, A. M. Testa, and A. Amore Bonapasta, *Phys. Rev. Lett.* **107**, 127206 (2011).
- ²¹DFT geometries were calculated in 64-atom supercells, with a cut-off energy of 400 eV and a $2 \times 2 \times 2$ Monkhorst-Pack grid for k-summation. HSE parameters were fixed to $\alpha = 0.25$ and $\mu = 0.25$, giving a GaAs band-gap $E_g = 1.42 \text{ eV}$.
- ²²A. L. Ankudinov, B. Ravel, J. J. Rehr, and S. D. Conradson, *Phys. Rev. B* **58**, 7565 (1998).
- ²³B. Ravel and M. Newville, *J. Synchrotron Radiat.* **12**, 537 (2005).